Food & Function

ROYAL SOCIETY OF CHEMISTRY

PAPER

View Article Online
View Journal | View Issue

Cite this: *Food Funct.*, 2026, **17**, 1336

Linking intestinal bitter taste receptors and GSPE-induced long-lasting benefits in ageing rats: an integrative analysis

Adrià Vilalta, Maria Descamps-Solà, Marta Sierra-Cruz, Alba Miguéns-Gómez, Raúl Beltrán-Debón, Esther Rodríguez-Gallego, Montserrat Pinent, Maria Teresa Blay, Anna Ardévol * and Ximena Terra

Ageing is associated with attenuated type-2 bitter-taste receptor (TAS2R) signalling and contributes to metabolic, inflammatory and barrier decline, but its system-wide impact along the gut remains undefined. We combined transcription analysis, physiology, metabolomics and microbiota profiling to test whether a brief grape-seed proanthocyanidin extract (GSPE) intervention can counter age-related dysfunction by long-term modulation of intestinal *Tas2r* expression. Female Wistar rats were distributed into young (2 months, n = 10) or aged (21 months, n = 24) groups; eleven aged animals received GSPE (500 mg kg^{-1}, oral gavage) for 10 days, followed by a 75-day wash-out. After sacrifice, we quantified Tas2r mRNA in five gut segments, assessed *ex vivo* permeability, enteroendocrine outputs, systemic metabolites, inflammatory markers, 16S microbiota and the untargeted plasma metabolome. An elastic-net/PLS-DA/random-forest pipeline ranked variables discriminating age and GSPE effects, and GeneNet partial correlations generated an integrated network. Ageing suppressed Tas2r gene expression across the small intestine and the distal colon, while the proximal colon was largely unchanged. Despite the long wash-out, the brief GSPE treatment restored small-intestinal Tas2r transcription of some receptors while paradoxically down-regulating a subset in the distal colon. Consensus variable selection highlighted enterohormone expression and its *ex vivo* secretion, intestinal barrier dysfunction indices, some microbiota genera and several Tas2r transcripts among the 34 strongest discriminators. Tas2rs formed high-betweenness hubs linking epithelial integrity, inflammatory tone and butyrate-producing taxa. These findings indicate that intestinal type-2 bitter taste receptors (Tas2rs) may integrate multisystem regulatory networks fundamental to healthy ageing. Brief administration of grape-seed proanthocyanidin extract (GSPE) is sufficient to durably reprogramme Tas2r expression and the surrounding microbiota–endocrine–barrier landscape in aged rats.

Received 30th July 2025,
Accepted 5th January 2026

DOI: 10.1039/d5fo03241e

rsc.li/food-function

1. Introduction

Bitter-taste receptors (TAS2Rs) are G-protein-coupled receptors first identified in lingual taste buds as sentinels for potentially harmful bitter compounds. Upon ligand binding, the receptor activates the heterotrimeric G-protein α-gustducin and its related downstream signalling, mainly through phospholipase Cβ2 activation, and triggers DAG and IP_3 production, leading to downstream intracellular Ca^{2+} increase.[1] TAS2Rs have diversified markedly across species, with up to 25 functional genes in humans and up to 35 in rodents, reflecting different ecological pressures. Although discovered in the oral cavity, *TAS2R* transcripts and proteins are now documented in the respiratory and gastrointestinal tracts, the brain and the immune system.[1,2] In these extra-oral sites, the receptors no longer serve conscious taste perception; instead, they participate in innate immunity, nutrient sensing, enteroendocrine regulation, smooth-muscle contractility and reproductive biology.[3]

Multiple lines of evidence indicate an age-related dampening of TAS2R bitter sensing and signalling. In a cohort of 1020 Europeans, intensity ratings for 6-*n*-propyl-thiouracil and other tastants declined steadily between 18 and 80 years, revealing loss of oral bitter sensitivity.[4] Senescence-accelerated SAMP1 mice show reductions in *Tas2r105* and its transducer α-gustducin within taste bud cells, indicating molecular and functional compromise of bitterness signalling.[5] Extra-orally, *T2R38* expression in peripheral lymphocytes is lower in elderly donors, suggesting systemic down-regulation of TAS2R

Universitat Rovira i Virgili, Departament Bioquímica i Biotecnologia, MoBioFood Research Group, C/Marcel·lí Domingo 1, 43007 Tarragona, Spain

signalling with age.[6] Although not all the reports on bitter-sensing and signalling produced consistent results, they mostly suggest that ageing modifies taste sensitivity.[7] We confirmed in the human gut, by real-time PCR profiling of basal *TAS2R* expression, that ageing up-regulates *TAS2R4*, *-5*, *-13* and *-20* in the descending colon, coinciding with increased GLP-1 release *ex vivo*. In contrast, key receptors such as *TAS2R38*, *-39* and *-42* showed low expression levels.[8] Our previous findings indicate that ageing does not universally lead to down-regulation of bitter taste receptor expression; however, its activation is linked to enterohormone secretion. In another study, we also demonstrated that metabolomic mapping further links colonic *TAS2R5* and *TAS2R38* expression to pro-inflammatory lipids, β-hydroxybutyrate and frailty markers in adults ≥60 years, underscoring functional impairment.[9] Collectively, the evidence suggests that TAS2R mRNA levels exhibit tissue- and receptor-specific ageing effects, while the system's signalling capacity tends to diminish. This supports the evaluation of pharmacological or dietary bitter ligands to transiently boost TAS2R activity and potentially mitigate age-related metabolic and inflammatory dysfunction.

Building on this premise, increasing life expectancy and the parallel rise in related comorbidities have highlighted the urgency for novel, mechanism-based interventions that can enhance metabolic health in older adults. TAS2Rs have been demonstrated to have a wide range of possible ligands which marks them as new targets for drug administration and novel therapies. Plant-derived polyphenols are attracting attention as stand-alone or adjuvant therapies because they combine a bitter sensory profile, suitable for TAS2R activation.[10] Among them, grape-seed proanthocyanidin extract (GSPE) is particularly compelling. Flavanols, the dominant phenolics in the human diet,[11] constitute the bulk of GSPE and have repeatedly been shown to protect rodents and humans against diet-induced obesity.[12–15]

We have demonstrated, in the gut of young rats, that GSPE strengthens the epithelial barrier, lowering permeability under obesogenic conditions,[13] and attenuates local oxidative and inflammatory markers such as myeloperoxidase (MPO) activity, while reducing systemic tumour necrosis factor (TNF)-α and C reactive protein (CRP).[15,16] It also modulates enteroendocrine secretion,[17] improves glucose homeostasis, increases brown adipose tissue size and metabolic activity,[18] and influences liver–muscle cross-talk.[19] Furthermore, our previous work in aged rats with the same extract showed that a 10-day pulse leaves measurable metabolic and microbiota benefits 11 weeks later: GSPE reduced food intake, visceral adiposity, HOMA-β and tumour incidence, mimicking caloric restriction, and blunted diet-induced disruptions in enteroendocrine secretion,[20–22] alongside a shift in the microbiota towards a younger profile long after the last dose.[23] Crucially, GSPE oligomers are poorly absorbed and cleared from the circulation within 24–48 h after extensive phase-II metabolism;[24,25] however, the physiological effects are still evident weeks later.[20–23]

Given the rapid clearance of GSPE oligomers alongside durable metabolic effects, the persistence of metabolic benefits suggests that early mucosal events initiate long-lasting adaptations. Candidate mediators include acute changes in epithelial barrier/immune tone (*e.g.*, reduced permeability,[12,13] MPO, and TNF-α/CRP[15,16]), enteroendocrine signalling (*e.g.*, GLP-1 and PYY[17]), and microbiota-dependent pathways;[23] however, the specific mediators remain to be established.

Intestinal TAS2Rs are expressed along the epithelium in mammals[26–29] and bind several bioactive molecules present in GSPE,[30,31] and upon activation of intestinal TAS2Rs, modulate enterohormone release[32–34] and immune tone,[35] aligning perfectly with the multisystem benefits observed after GSPE administration. Because the TAS2R genotype[36] and individual differences in microbiota-mediated flavanol catabolism[37] strongly influence responsiveness to bitter ligands, strategically timed GSPE 'pulses' could be tailored to a person's genetic and microbial profile—placing this approach squarely within the scope of personalised nutrition.

Taken together, these data support the concept that intestinal TAS2Rs act as a molecular bridge linking luminal polyphenols with systemic metabolic and immune outcomes in ageing. We therefore hypothesise that a short-term GSPE exposure induces long-lasting changes in Tas2r gut expression that remain detectable 11 weeks later in aged rats. Here, we test this idea by examining whether GSPE modulates intestinal *Tas2r* expression and whether these Tas2r transcripts show associations with age-associated metabolic decline. Finally, we use integrative machine-learning analysis to pinpoint the variables most predictive of successful ageing and the contribution of Tas2r signalling to that phenotype.

2. Materials and methods

2.1. Proanthocyanidin extract

The grape seed extract rich in proanthocyanidins (GSPE) was obtained from Les Dérivés Résiniques et Terpéniques (Dax, France). According to the manufacturer, the GSPE used in this study (lot 207100) had a total proanthocyanidin content of 76.9% consisting of a mixture of monomers of flavan-3-ols (23.1%), dimers (21.7%), trimers (21.6%), tetramers (22.2%) and pentamers (11.4%).

2.2. Experimental design

A total of 36 female Wistar rats were acquired from Envigo (Barcelona, Spain). The rats were of different ages, with the young group being 2 months old (n = 10) and the rest of the animals aged 21 months (n = 26). After one week of adaptation, all rats were individually housed under controlled conditions (22 °C, 12-hour light/dark cycle) and were fed *ad libitum* with a standard chow diet (Teklad 2014, Envigo, Barcelona, Spain) for the duration of the whole experiment.

After the period of acclimation, the aged rats were randomly distributed into two experimental groups: aged (n = 14) and aged supplemented with GSPE (n = 12). The GSPE group received an oral dose of GSPE at 500 mg per kg b.w. (body weight) for 10 consecutive days (Fig. 1). To ensure a fasting state, food was removed three hours before the onset of the

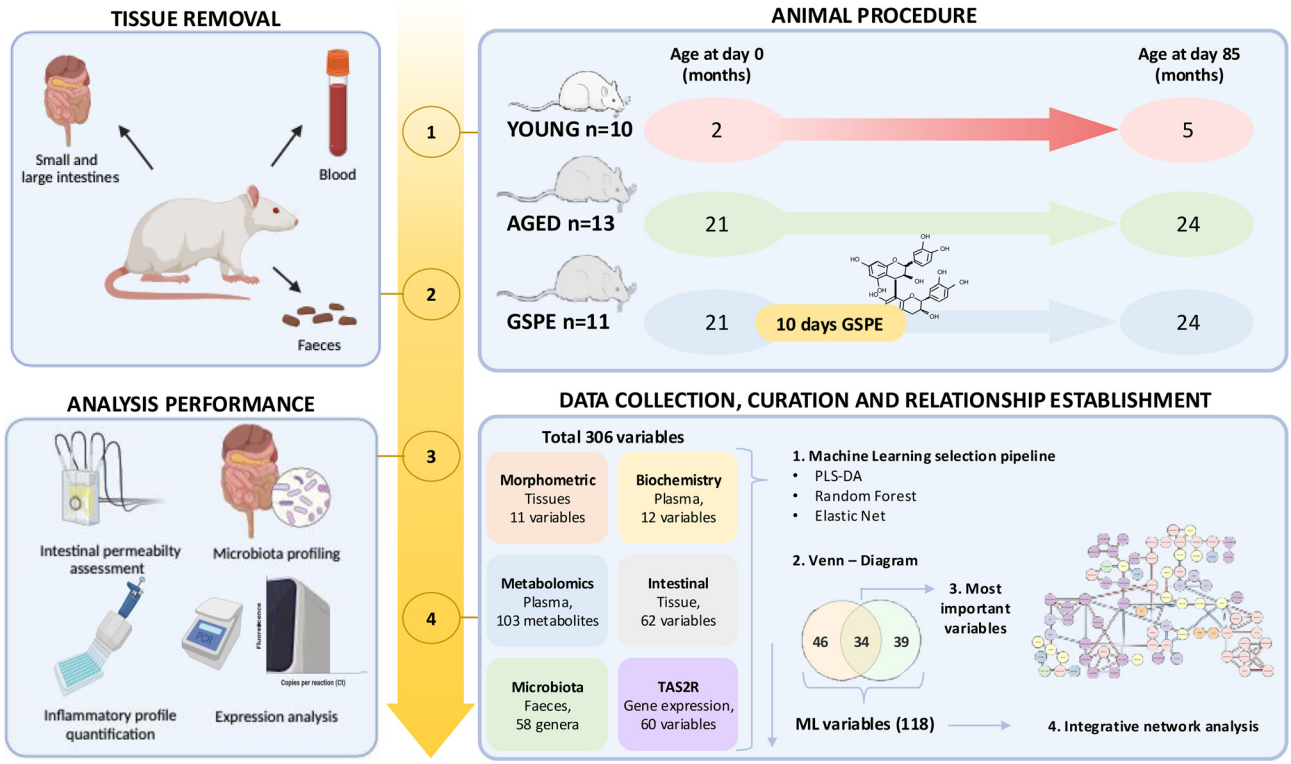

Fig. 1 Experimental design. The study comprised ten 2-month-old (young) rats and twenty-four 21-month-old (aged) rats, of which 11 aged animals received GSPE (500 mg kg^{-1}) by oral gavage for 10 days. After treatment, the animals were maintained for an additional 75 days before being sacrificed, and tissues (intestine, blood, and faeces) were collected. Permeability assays, microbiota profiling, inflammatory and enterohormone quantification, and gene expression analysis were performed. The collected data were analysed using machine learning software to identify the most important variables, followed by a partial correlation network analysis to reveal relationships between variables.

dark cycle, and GSPE was administered *via* oral gavage one hour prior to the dark cycle, dissolved in tap water. Control animals received tap water as the vehicle. Food was replenished immediately after gavage.

Following the supplementation period, all animals were maintained caged for 75-day wash-out with a renewed chow diet and free access to tap water. The duration of the wash-out was selected to eliminate any direct pharmacological exposure, based on human and rat ADME data indicating plasma clearance within 1–3 days and no tissue accumulation even after long-term administration.[25,38]

Body weight records were monitored every two weeks. During the study, one aged rat died spontaneously and one GSPE rat died due to procedure-related complications, resulting in final group sizes of young (n = 10), aged (n = 13), and GSPE (n = 11).

All procedures were approved by the Experimental Animal Ethics Committee of the Generalitat de Catalunya, Spain (Department of Territory and Sustainability, General Directorate for Environmental and Natural Policy, project authorization code: 10183).

2.3. Blood and tissue collection

The rats were fasted for 12 hours before euthanasia. After sacrifice, plasma and intestinal samples from the duodenum, jejunum, ileum, proximal and distal colon along with other internal tissues/organs such as the liver, kidneys, spleen, different adipose tissues (gonadal, mesenteric, subcutaneous, retroperitoneal and brown), stomach, right femur, caecal contents and caecum were rapidly removed, weighed and frozen in liquid nitrogen before storage at −80 °C until further analysis.

2.4. Biochemical variables

Commercial colorimetric enzymatic kits were used to measure levels of glucose, triacylglycerol (TAG), cholesterol, urea, and creatinine (QCA, Tarragona, Spain), non-esterified fatty acids (NEFAs) (Wako, Neuss, Germany) and β-hydroxybutyrate (Ben Biochemical Enterprise, Milano, Italy) in the plasma samples in accordance with the manufacturers' instructions. Commercial ELISA kits were used to quantify plasma levels of insulin (Millipore, Madrid, Spain) and glucagon (Mercodia, Uppsala, Sweden).

2.5. Real-time expression analysis

Total RNA was extracted from each intestinal segment using TRIzol reagent (Thermo Fisher Scientific, Waltham, MA, USA), following the phenol–chloroform extraction method. Complementary cDNA was obtained using the high-capacity

cDNA reverse transcription kit (Applied Biosystems, Madrid, Spain), following the manufacturer's instructions.

Quantitative PCR amplification was performed using TaqMan Universal PCR Master Mix (Applied Biosystems, Madrid, Spain) and specific TaqMan probes for the r*Tas2r108* (Rn02396427_s1), r*Tas2r119* (Rn00576950_s1), r*Tas2r126* (Rn00595098_s1), r*Tas2r135* (Rn02585807_s1), r*Tas2r137* (Rn01500928_s1), r*Tas2r138* (Rn02396417_s1), r*Tas2r139* (Rn04218919_s1), r*Tas2r140* (Rn01492598_s1), r*Tas2r143* (Rn02585801_s1) and r*Tas2r144* (Rn02585844_s1) genes from Thermo Fisher Scientific (Waltham, MA, USA). The relative expression of each gene was compared with the aged group using the $2^{-\Delta\Delta Ct}$ method and with cyclophilin (PPIA) (Rn00690933_m1) as the endogenous gene and the aged group as the relative control.

2.6. Statistical analysis (gene expression)

Relative expression results are expressed as mean ± standard error of the mean (SEM). The Mann–Whitney nonparametric statistical test was assessed comparing the young and GSPE groups with the aged group. Analyses were performed using SPSS software version 27 (IBM, Chicago, USA). p-Values <0.05 were considered statistically significant.

2.7. Metabolomics from plasma

The extraction of plasma metabolites was performed using gas chromatography coupled with quadrupole time-of-flight (GC-qTOF). For the extraction, protein precipitation extraction was performed by adding eight volumes of methanol : water (8 : 2, v/v) containing an internal standard mixture (succinic acid-d4, myristic acid-d27, glycerol-13C3, D-glucose-13C6, α-ketoglutaric acid-13C4 and metabolomics labelled amino acid mixture) to plasma samples. Then, the samples were mixed, incubated at 4 °C for 10 min, and centrifuged at 15 000 rpm, and the supernatant was evaporated to dryness before compound derivatization (methoximation and silylation). The derivatized compounds were analysed by GC-qTOF (model 7200 of Agilent, USA). The chromatographic separation was based on the Fiehn method, using a J&W Scientific HP5-MS 30 m × 0.25 mm i.d., 0.25 μm film capillary column and helium as the carrier gas using an oven program from 60 to 325 °C. Ionization was performed by electronic impact (EI), at an electron energy of 70 eV operating in full-scan mode. In addition to targeted compounds from central carbon metabolism, which were quantified using internal standard calibration curves, a screening for the identification of more metabolites was performed by matching their EI mass spectra and retention times to the Fiehn metabolomics library (from Agilent), which contains more than 1400 metabolites. After putative identification of metabolites, these were quantified and expressed in μM. For statistical analyses, those metabolites that were present in 100% of the samples in all groups were considered. Ninety-five metabolites were identified in all plasma samples.

2.8. Other variables

Microbiota data (only at the genus level for analysis simplification), intestinal dysfunction and enterohormone assessment *ex vivo*, and SCFA quantification have already been described in ref. 22, 23 and 39–41.

2.9. Variable importance ranking

To rigorously delineate differences between groups, variables exhibiting the greatest discriminatory power were selected, using the following machine-learning pipeline. All data processing, integration, variable selection pipeline and statistical analysis described in this section were performed using R version 2023.09.0+463. Previous data from plasma metabolomics, biochemical measurements, morphometric measurements from collected tissues, microbiota data and SCFA quantifications were integrated with the 12 *Tas2r* expression in 5 gut segments. Preprocessing steps included median imputation for missing values and removal of redundant variables to reduce the dimensionality and collinearity of the data. The resulting integrated data consisted of 85 variables which included biochemical, inflammatory, enterohormone, SCFA and permeability variables, 103 metabolomic variables, 58 microbiota variables and 60 variables of *Tas2r* expression. The data were centred and scaled by dividing each variable by its standard deviation.

The variables were further analysed using a multivariate approach by our variable selection pipeline that takes consensus of three methods: elastic net regression, partial least squares-discriminant analysis (PLS-DA), and random forest (RF). The parameters for each of the methods were optimized with 100× repeated 5-fold cross-validation following the one standard error rule using the glmnet R package. The measures of variable importance were calculated from the final models with the optimized parameters. Non-zero coefficients of a subset of variables selected from the elastic net model, variable importance in projection (VIP) coefficients provided by the PLS-DA model, and mean decrease in Gini values calculated by the RF model were used as measures of variable importance. Variables selected by the elastic net were defined as the variables with non-zero coefficients. Variable selection for PLS-DA and RF was performed by ranking the variables based on the corresponding variable importance measure and taking the ones above the elbow point. The size of the largest set among the three selected variable sets was taken as a score for the most important variable in each set. The other variables in each set were scored in decreasing order according to their corresponding variable importance measures within the sets. The scores were summed across the sets to obtain total scores for the variables. The most important variable in consensus would be the variable selected with most of the methods, with the highest variable importance measure in each method, and would have the highest total score.

2.10. Partial correlation network

The selected variables were cross-referenced using the Venn diagram package. Partial correlation was calculated between

the variables selected from at least one of the three methods for ageing and GSPE effect comparisons, using the GeneNet R package. These correlations were plotted using Cytoscape version 3.10.0. Pair-wise correlations were then recomputed for the important clusters retained in the partial-correlation graph by using the two-tailed Spearman ρ coefficient. Although partial correlation isolates direct associations after conditioning on the rest of the variables, a concordant Spearman sign and $P < 0.05$ indicate that the same relationship is also evident in the raw data (any edge changed sign or lost significance), lending robustness to the inference (SI Tables S2–S10).

3. Results

3.1. Expression profile of *Tas2r* in aged rats

We deliberately imposed a 75-day wash-out (7.5 times the treatment length) to test whether a brief exposure to proanthocyanidins could generate long-lasting physiological reprogramming once the parent compounds had cleared.

Our results reveal an age-related decline in the intestinal expression of bitter-taste receptors that is region specific. The largest decreases occurred along the small intestine (Fig. 2A–C), while the proximal colon showed no consistent age effect (Fig. 2D), and no receptor showed age-related up-regulation in our dataset. Specifically, *Tas2R119*, *Tas2R126*, *Tas2R135*, *Tas2R137*, *Tas2R138*, *Tas2R140* and *Tas2R143* decreased significantly in at least two small-intestinal segments. In contrast, expression in the proximal colon remained unchanged (Fig. 2D). The distal colon, however, mirrored the small-intestinal profile, showing comparable down-regulation (Fig. 2E). Of particular interest, *Tas2R119*, *Tas2R126* and *Tas2R135* were consistently reduced across both the small intestine and distal colon in aged rats, underscoring a region-spanning attenuation of gut bitter-taste receptor expression with age.

Globally, GSPE administration clearly increased the expression of Tas2r in the small intestine and the proximal colon (Fig. 2A–D), except the expression of duodenal receptor *Tas2r139*, which was significantly reduced (Fig. 2A). In contrast, GSPE in the distal colon appears to exert an opposite effect, as evidenced by a reduction in the expression levels of *Tas2r138*, *Tas2r139*, *Tas2r143*, and *Tas2r144* (Fig. 2E).

3.2. Variable selection by machine-learning tools

We have previously demonstrated that this rodent ageing model approximates key features of age-related metabolic disruption in humans. In light of our previous results, we now delve deeper into the role of Tas2rs through the analysis of their relationships with the phenotype of aged rats.

For that, all the expression levels of bitter taste receptors throughout all the intestines were combined with all previously collected data (SI Table S1). All the data were analysed using three different approaches for variable importance analysis: elastic net, random forest, and PLS-DA. The results were later combined into a ranked list where the variables with higher rankings exhibited greater power in the discrimination of the groups. Due to the nature of the analysis, only one condition, ageing or GSPE treatment, was analysed at a time.

Enterohormone variables, including *Chromogenin A* (*Chga*) expression in the colon or secreted Cholecystokinin (CCK), followed by adiposity levels, ileal secretion of Glucagon-Like Peptide-1 (GLP1) (*ex vivo*) and *Peptide YY* (*Pyy*) expression in the proximal colon among other several variables, exhibited the highest power in differentiating between the young and aged groups (Fig. 3A). Among the 72 selected variables, in the top 20 variables, the expression of bitter taste receptors (135 in the distal and proximal colon, 119 in the ileum and 144 in the proximal colon), along with morphometric parameters and some plasma metabolites, were also present. As anticipated, variables exhibiting significant changes between the young and aged groups appear at the top of the importance ranking. Beyond these primary markers, several additional variables displayed appreciable discriminative power, despite their comparatively subtle changes.

When the GSPE group was compared solely to the aged group, only 54 variables were selected. The top 20 selected variables included again a large number of enterohormone variables. Moreover, in this comparison, *ex vivo* measurements of intestinal integrity such as transepithelial permeability (TEER) in the ileum or the transport of fluorescein isothiocyanate-dextran (FITC-D) and the expression of tight junction proteins appear within the top selected variables. Interestingly, microbiota variables also gained power in this comparison (Fig. 3B). *Tas2r* expression was also present in this selection (138 and 144 in the proximal colon, 144 in the distal colon and 119 in the ileum).

To start curating the important variables, we drew a Venn diagram to identify the variables that were selected in both comparisons. Only 34 variables were common among the 92 variables selected through the machine-learning process (Table 1). The importance scores from the variables were then normalised to make them comparable, and the variables were ranked again.

Table 1 shows the variables that best describe the ageing scenario together with the GSPE effect. The expression of *Chga* and *Pyy* in colon samples had the highest scores in this selection process. Notably, the expression of *Tas2r119* and *144* in the ileum and proximal colon, respectively, emerged in the third and fourth positions. Other Tas2rs that appeared in these common variables were *135*, *138*, *139*, *143* and *144* in the colonic tissue and *Tas2r108* in the ileum. Other variables selected comprise the expression and *ex vivo* secretion of certain enterohormones, plasma levels of urea, osteocalcin and insulin; inflammatory and gut integrity parameters; and some microbiota species. A notable finding was the opposite behaviour exhibited by most of the selected variables when comparing the aged group and the GSPE group (Table 1).

To check the accuracy of this methodology, we compared the performance of 3 Principal Component Analysis (PCA) including the different sets of variables (Fig. 4): (1) all the variables in our study; (2) variables selected by machine learning tools; and (3) the selection of variables obtained from the Venn diagram, which include the common variables selected

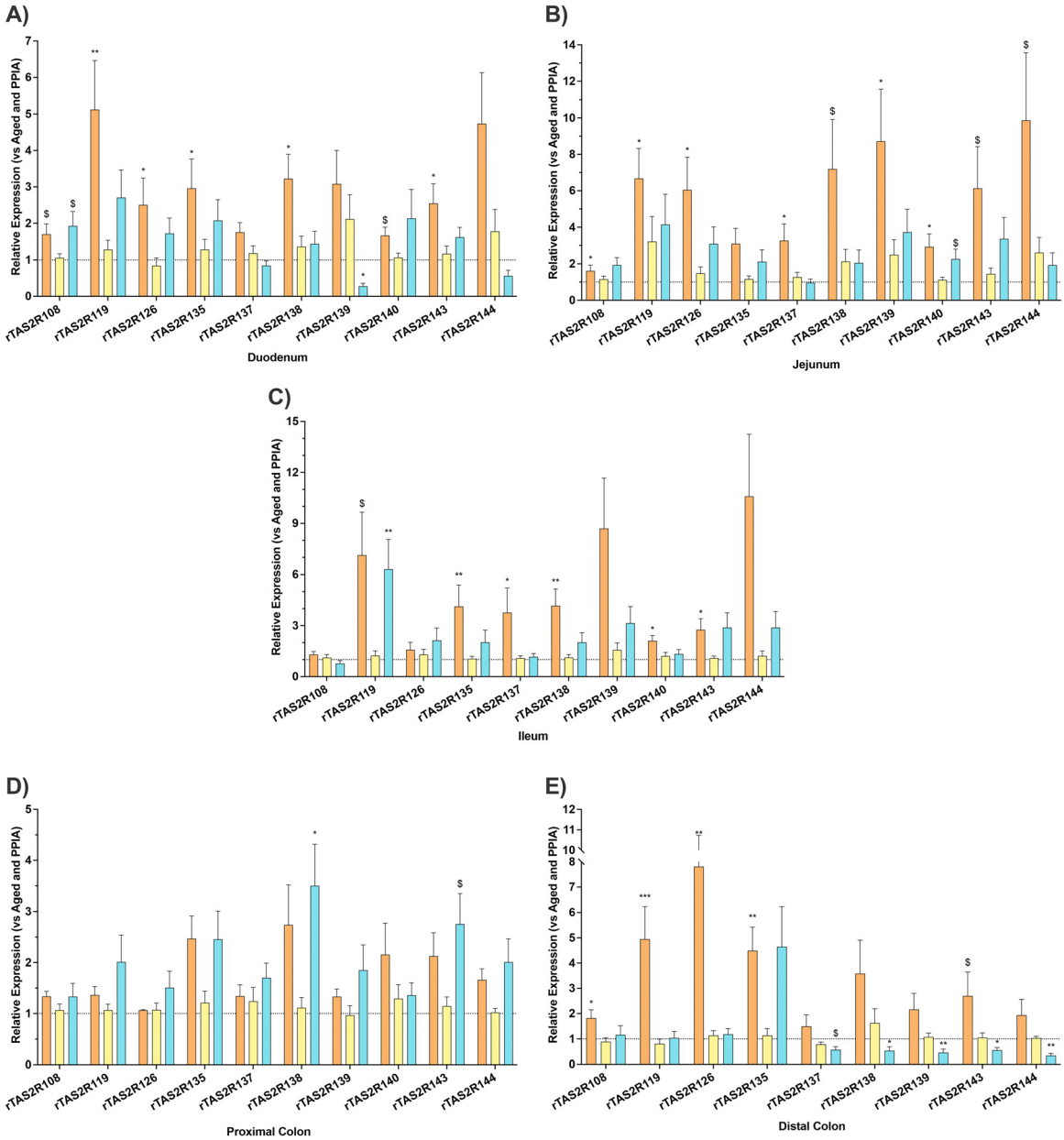

Fig. 2 Relative expression of bitter taste receptors through the gastrointestinal tract. Expression was normalized to PPIA and calculated using the $2^{\Delta\Delta Ct}$ method using the aged group as the relative control. Bars represent the mean ± SEM (n = 10 rats per group). Different colours represent different experimental groups: orange for young, yellow for aged, and blue for GSPE-treated. Statistical significance was determined using the Mann–Whitney non-parametric statistical test. \$ $p < 0.1$, * $p < 0.05$; ** $p < 0.01$, *** $p < 0.001$ *vs.* aged group.

in the young *vs.* aged and aged *vs.* GSPE analyses. In the first PCA (Fig. 4A), we could observe a differentiation between the aged groups and the young groups but with a significant overlap between the aged and the GSPE groups. When we took the variables that were selected in our refinement process (Fig. 4B), we observed a differentiation between the groups and an increase in the coverage of the axis. Lastly, when only the common variables from the Venn diagram were selected, the separation between groups and the coverage were increased, with almost no overlap (Fig. 4C). The separation of the groups when reducing the number of variables proved that the selection methodology was effective.

3.3. Partial correlation network topology of the integrated dataset

To move beyond single-variable ranking and probe how the features interact as a system, we calculated a partial-correlation matrix on the full, cleaned dataset and rendered the significant associations as a network. This approach allows us to visualise putative direct links among microbiota, metabolites,

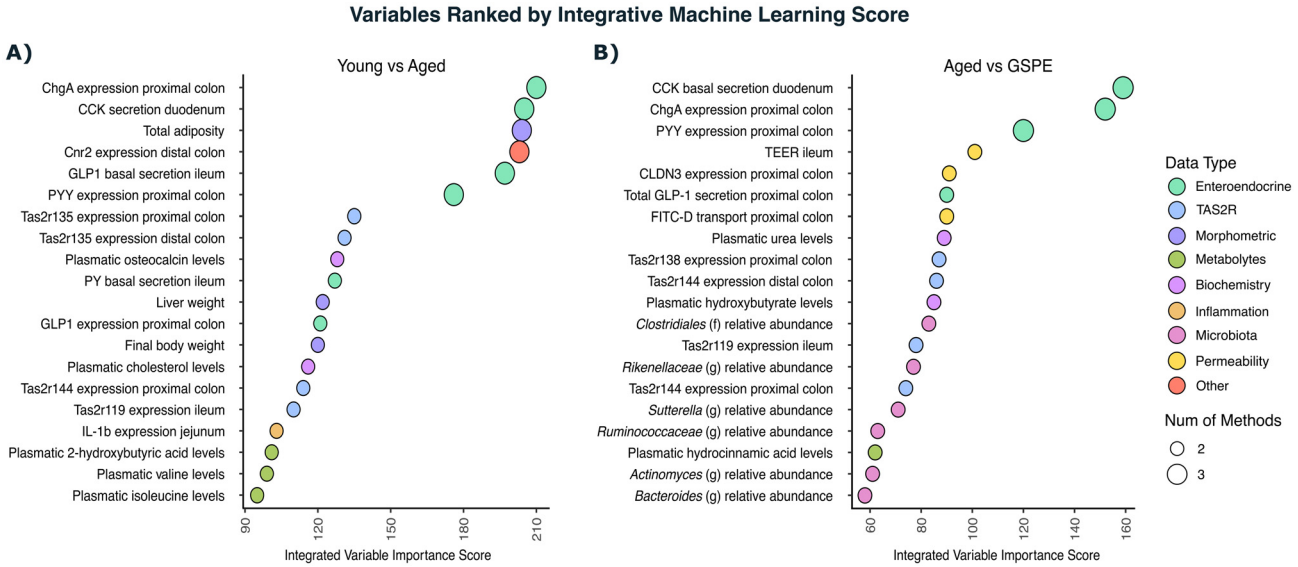

Fig. 3 Importance variable score plot. (A) Most important variables selected between the young and aged groups. (B) Most important variables selected between the aged and the GSPE groups. Each colour represents a different category, and the size of the ball represents the number of methods used to select the variables. Higher values indicate greater power in discriminating between groups.

barrier markers and Tas2r transcripts. The topology of this network, detailed below, provides a coherent map of how variables coalesce into functional clusters.

After filtering the partial-correlation matrix for q value <0.05, the network visualised in Fig. 5 contained 98 nodes and 151 edges. Seven thematic blocks are recognisable: microbiota genera, *Tas2r* transcript levels, plasma metabolites, classical plasma biochemistry-enterohormones, body/tissue weights (purple), and intestinal barrier-inflammation read-outs.

The *Tas2r* family dominated the core of the network and segregated according to gut segment. In the ileum, *Tas2r108*, *-118*, *-137* and *-138* mRNAs formed a fully connected clique that was positively linked to *Bifidobacterium* (g), indicating that higher ileal expression of these bitter-taste receptors co-occurred with increased abundance of this genus. A second densely connected module integrated *Tas2r119*, *Tas2r144* and *Tas2r135* mRNA expression in the proximal colon. These transcripts correlated positively with transepithelial electrical resistance in the colon and showed an indirect, negative association with duodenal *Mylk* expression *via* intermediate nodes, consistent with an association between higher receptor expression and improved epithelial integrity. In the duodenum, *Tas2r119* expression showed a positive correlation with circulating D-xylose. Through this metabolite, the receptor was indirectly and inversely related to jejunal *Interleukin 1b* (*Il1b*) mRNA, whereas duodenal expression of *Tas2r143* was inversely related to the bone-resorption marker CTX-I and positively with hippuric acid.

Microbiota nodes were frequently positioned at the interface between host and metabolite clusters. *Coprococcus* was positively connected with the expression of *proglucagon* (*Gcg*) in the proximal colon and with *Tas2r140* expression in the same segment, while *Prevotella* showed a positive link to jejunal *Tnf* expression, suggesting taxon-specific relationships with pro- or anti-inflammatory tone. A sub-network centred on *Clostridiales* (family level) included positive edges to plasma insulin and uric acid and extended to *Bilophila* and *Oscillospira*, hinting at a microbiota–metabolic axis that tracks insulin dynamics.

Barrier and permeability markers lay in a compact, largely negative cluster. Both FITC-D, in the colon and ileum, displayed inverse correlations with a series of aromatic and purine metabolites (hippuric, hydrocinnamic and vanillylmandelic acids, and uric acid), which are involved in microbial metabolism, oxidative stress regulation, and inflammation. In contrast, FITC (colon) was positively related to *Streptococcus*, D-mannonic acid and D-arabinose. Together with the TEER (colon)/Myosin light chain kinase (*Mylk*) (mRNA duodenum) relationships described above, these edges point to distinct metabolite–microbe patterns accompanying either tightened or loosened barrier function.

Within the metabolome, branched-chain amino acids (isoleucine, leucine, and valine) formed an isolated triangle of positive correlations. Oleic acid and ornithine were negatively linked to *Mylk* expression in the duodenum and *Interleukin-6* (*Il6*) expression in the jejunum, respectively, and positively to glycerol, suggesting a small lipid–amino acid sub-network with anti-inflammatory overtones.

Finally, systemic metabolic read-outs showed partial correlations onto body-weight nodes: final body weight correlated positively with plasma cholesterol, which in turn related to liver mass, delineating a simple weight–lipid module disconnected from the intestinal clusters. Overall, the integrative network highlights strong intra-segmental co-regulation of *Tas2r* genes, specific bacterial genera that covary with bitter-

Table 1 Overlapping variables identified by both selection methods in young *vs.* aged and aged *vs.* GSPE comparisons

Variable	Type (units)	Tissue	Ageing *vs.* young	GSPE *vs.* ageing
Chga	mRNA (2^{-DDCt})	Proximal colon	Down	Up
Pyy	mRNA (2^{-DDCt})	Proximal colon	Down	Up
Tas2r119	**mRNA (2^{-DDCt})**	**Ileum**	**Down**	**Up**
Tas2r144	**mRNA (2^{-DDCt})**	**Proximal colon**	**Down**	**Up**
GLP-1 basal	Metabolite (pM)	Ileum *ex vivo*	Up	Up
FITC-dextran	Permeability marker (mM)	Proximal colon *ex vivo*	Down	Up
CCK stimulated	Metabolite (ng mL^{-1})	Duodenum *ex vivo*	Up	Down
Tas2r135	**mRNA (2^{-DDCt})**	**Proximal colon**	**Down**	**Up**
CTXI	Metabolite (ng mL^{-1})	Plasma	Down	Up
Urea	Metabolite (mM)	Plasma	Down	Up
GLP1	Metabolite (pM)	Colon *ex vivo*	Down	Down
Tas2r135	**mRNA (2^{-DDCt})**	**Distal colon**	**Down**	**Up**
Osteocalcin	Metabolite (ng mL^{-1})	Plasma	Down	Up
Claudin3	mRNA (2^{-DDCt})	Proximal colon	Up	Down
MPO	Activity (mU)	Jejunum	Up	Down
Rikenellaceae	Microbiota genus (relative abundance)	Caecal content	Up	Down
Insulin	Metabolite (pM)	Plasma	Up	Down
FITC-dextran	Permeability marker (mM)	Ileum *ex vivo*	Up	Up
Actinomyces	Microbiota genus (relative abundance)	Caecal content	Down	Up
TEER	Resistance (W cm^2)	Ileum *ex vivo*	Up	Down
Tas2r139	**mRNA (2^{-DDCt})**	**Proximal colon**	**Down**	**Up**
Tas2r138	**mRNA (2^{-DDCt})**	**Proximal colon**	**Down**	**Up**
Tas2r144	**mRNA (2^{-DDCt})**	**Distal colon**	**Down**	**Down**
Tnf	mRNA (2^{-DDCt})	Jejunum	Down	Down
Tas2r143	**mRNA (2^{-DDCt})**	**Proximal colon**	**Down**	**Up**
Tas2r108	**mRNA (2^{-DDCt})**	**Ileum**	**Down**	**Up**
Decanoic acid	Metabolite (mM)	Plasma	Up	Up
Bilophila	Microbiota genus (relative abundance)	Caecal content	Up	Down
Tas2r138	**mRNA (2^{-DDCt})**	**Ileum**	**Down**	**Down**
HOMA IR	Ratio	Plasma	Up	Down
Mylk	mRNA (2^{-DDCt})	Duodenum	Down	Up
TEER	Resistance (W cm^2)	Proximal colon *ex vivo*	Up	Up
Anaerotruncus	Microbiota genus (relative abundance)	Caecal content	Down	Up

Variables are listed in decreasing order of importance for group separation. Each entry includes the variable name, units, tissue of origin, and direction of change relative to the aged group. Bitter taste receptors are highlighted.

taste receptor expression and inflammatory transcripts, and discrete metabolite constellations that track epithelial integrity and systemic metabolic status. Taken together, these patterns assign the intestinal *Tas2r* transcripts a bridging role: they interface epithelial integrity, inflammatory tone, enteroendocrine outputs and microbial ecology, providing a mechanistic backbone for the multiorgan benefits previously observed after GSPE administration in aged rats.

4. Discussion

Our earlier studies demonstrated that grape-seed proanthocyanidin extract (GSPE) exerts geroprotective effects across several hallmarks of human ageing. Building on that foundation, we have now pooled all available datasets (enterohormone outputs, morphometric indices, *in vivo* and *ex vivo* barrier read-outs, plasma metabolomics, systemic inflammatory markers, short chain fatty acids, 16S-based microbiota datasets and untargeted plasma metabolites) together with the newly quantified *Tas2r* transcriptome to explore the potential contribution of intestinal bitter-taste receptors to healthy ageing.

Age-associated attenuation of bitter-taste signalling has been documented in both humans and rodents, yet most reports focus on lingual tissue or isolate single intestinal segments.[42,43] Importantly, by 'attenuation' we refer to functional signalling capacity; at the transcript level, our data show segment-specific effects. Reduced taste perception is often assumed to involve changes at the molecular level, such as decreased Tas2r expression in taste bud cells, yet this link remains largely unsubstantiated in current research. Evidence for *Tas2r* expression in extra-oral tissues remains limited, and investigations that relate this expression to functional signal-transduction outcomes are even scarcer. In our work, we found that ageing reshaped the intestinal bitter-taste landscape in rats: most *Tas2r* transcripts decreased sharply from the duodenum to the ileum and again in the distal colon, whereas the proximal colon was broadly preserved (no consistent change). A similar segment-specific pattern has been described in humans, where jejunal *Tas2r* expression declines with age while several colonic receptors rise or remain stable;[8] it also resonates with the well-known drop in sensory taste acuity that begins in mid-life.[4,5,7,42,43] Because extra-oral TAS2Rs help tighten epithelial junctions, restrain nuclear factor-kB (NF-kB) and promote enteroendocrine hormone release,[1,35] their

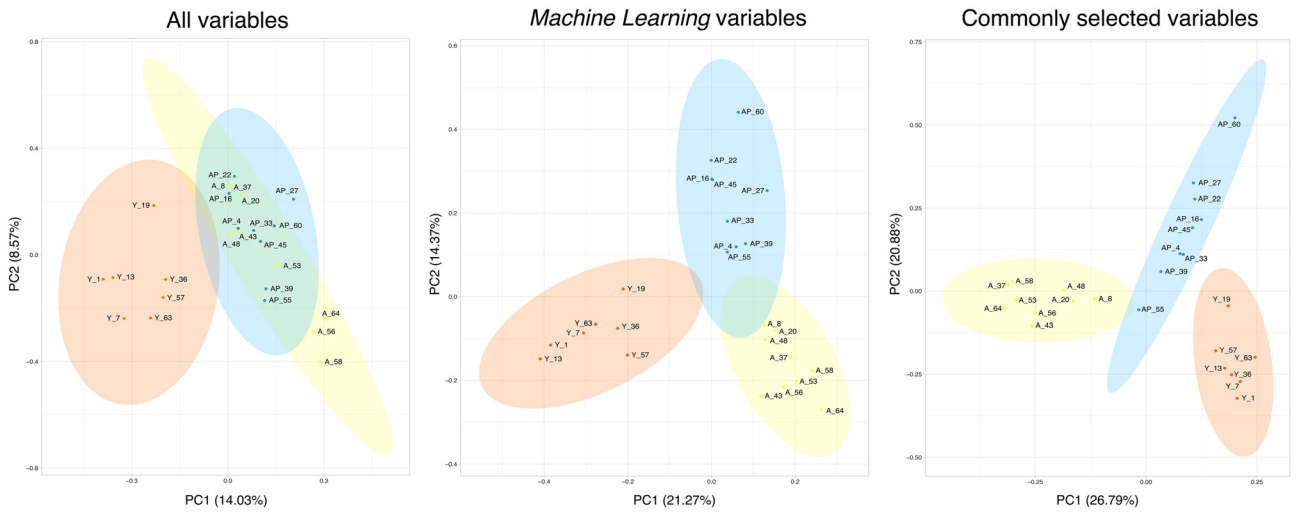

Fig. 4 Principal component analysis (PCA). (A) Using all variables; (B) using variables selected by machine learning; and (C) using variables common to both machine learning selection methods. Each dot represents one rat. Each colour represents a different experimental group: orange for young, yellow for aged, and blue for GSPE-treated. Axes represent the first two principal components, with the percentage of explained variance indicated. Ellipses represent 95% confidence intervals for each group. PCA was performed using R version 2023.09.0+463.

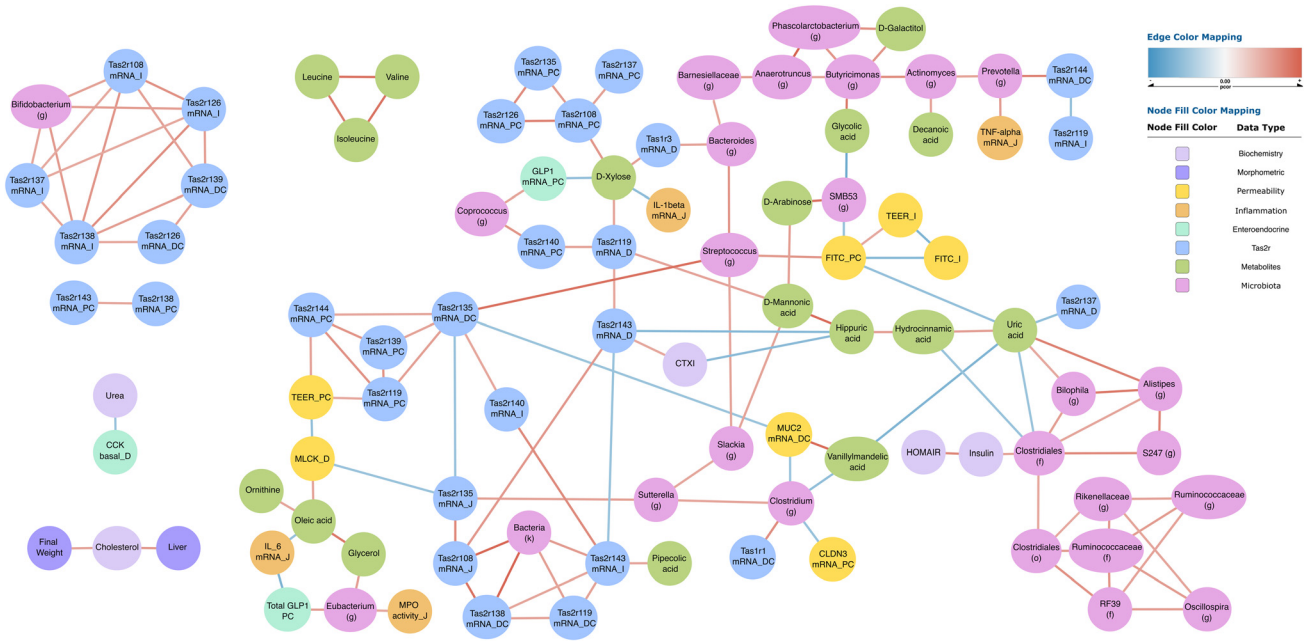

Fig. 5 Partial correlation network of machine learning-selected variables. Nodes represent individual variables, and edges indicate significant partial correlations (q-value <0.05). Red edges denote positive correlations, while blue edges indicate negative correlations; edge intensity reflects the strength of the correlation. Node colors correspond to variable categories: blue = Tas2r expression, light purple = biochemical variables, dark purple = morphometric variables, yellow = permeability, orange = inflammatory parameters, turquoise = enterohormones, green = metabolites, pink = microbiota variables, and red = other variables. Tissue origins are indicated by letters: D = duodenum, J = jejunum, I = ileum, PC = proximal colon, and DC = distal colon.

decrease could represent a potential mechanism underlying barrier leakiness, low-grade inflammation and altered incretin tone that often accompany senescence, although a direct causal relationship has not yet been established.

A preventive ten-day treatment with GSPE largely maintained higher *Tas2r* expression along the small intestine and proximal colon but reduced several receptors distally. This seemingly paradoxical response makes biochemical sense. Oligomeric flavan-3-ols in GSPE activate broadly tuned receptors such as TAS2R14 and 39,[44] but are poorly absorbed and therefore reach the colon almost intact, where the microbiota converts them into hippurate, pipecolate and related metab-

olites.[45] Proximal segments thus encounter parent agonists and mount a transcriptional up-swing, whereas distal tissues face a mixed pool of agonists and high local metabolite concentrations, a context that can trigger feedback repression.

Although these processes might take place during GSPE treatment, circulating flavan-3-ols and their phase-II and microbiota-derived metabolites exhibit rapid clearance *in vivo*.[24,25] In humans, radiolabelled (−)-epicatechin is >90% recovered in excreta within 48 h, and plasma radioactivity falls below quantification by 36–72 h.[38] In rats, even after 12 weeks of daily GSPE, LC-MS/MS profiling 21 h after the last dose shows no tissue accumulation of flavanol metabolites, indicating effective elimination at each dosing cycle.[25] Given this short systemic half-life and lack of tissue storage, our 75-day wash-out far exceeds known exposure windows, arguing against residual ligand-driven TAS2R activation at the time of sampling. Our data therefore support an 'imprinting' model: early receptor activation, coupled with polyphenol-driven shifts in microbial ecology, sets off a cascade that maintains higher *Tas2r* transcription, tighter epithelia and a rejuvenated enteroendocrine profile weeks after the last dose. As stated before, the preventive effects of GSPE have been documented in previous studies, which demonstrated its epigenetic potential in young rats subjected to an obesogenic challenge. Notably, the protective effects persisted even after a 17-week washout period following a short 10-day treatment.[15,46]

Using three independent machine-learning algorithms, we asked which among >300 variables best separated groups. For both ageing and the GSPE effect, enterohormone variables (*Chga* and *CCK*) prevailed over other variables. However, for the GSPE effect, permeability variables gained importance, ranking among the top ten variables. Regarding bitter taste receptors, the expression of *r135* in the colon (both proximal and distal), *r144* in the proximal colon, and *r119* in the ileum were among the top twenty most important variables. The variables consistently maintained for the GSPE effect were *r119* in the ileum and *r144* in the proximal colon, with the addition of r138 in the proximal colon and *r144* in the distal colon. As expected, when both datasets were integrated, the third and fourth variables with the highest discriminatory power were ileal *r119* and *r144*, followed by *r135*, *r139*, *r138*, *r144*, and *r143*, mainly in proximal and distal colonic tissues. Interestingly, the expression of all these receptors decreased with ageing, whereas GSPE administration preserved their previous expression levels, increasing them compared with the aged group in almost all cases. The human homologues of these receptors are *TAS2R1* for *Tas2r119*, *TAS2R60* for *Tas2r135*, and *TAS2R40* for *Tas2r144*.[1] In humans, several studies have reported associations between bitter taste receptors and ageing, primarily focusing on the decline in taste perception[4] and the investigation of polymorphisms in TAS2R16, TAS2R4, TAS2R5,[47] and TAS2R38 [48] genes in relation to longevity. Moreover, the expression levels of TAS2R5 and TAS2R38 have been found to correlate with proteins involved in the inflammatory response and with liver function, respectively.[9] When we mapped all variables into a partial-correlation graph, the same bitter receptors sat at the crossroads of four functional domains: epithelial integrity, inflammation, enteroendocrine output and microbiota.

In the ileum, a tightly knit quartet of *Tas2r108/118/137/138* was connected to an expansion of *Bifidobacterium*, a genus known to generate flavanol metabolites and reinforce the barrier.[23,49] Proximal-colonic *Tas2r119* and *144* were positively linked to transepithelial electrical resistance and, through intermediate nodes, negatively to duodenal *Mylk*, underscoring a scenario in which stronger bitter tone tracks with tighter epithelia. The mirror image appeared in the permeability cluster: FITC-D flux travelled with *Streptococcus* abundance; pathogenic streptococci disrupt junctions *via* streptolysin-S,[50] while exopolysaccharides from probiotic strains can counteract the damage.[51] GSPE simultaneously boosted *Tas2r* expression and decreased the abundance of *Streptococcus*, suggesting a dual route by which the extract reinsulates the ageing gut.

Endocrine signals fitted seamlessly into this architecture. *Coprococcus* and *Tas2r140* converged on GLP-1 in the proximal colon. Bitter agonists such as denatonium stimulate GLP-1 release *via* TAS2R-PLC pathways;[34] short-chain fatty acids from butyrate producers like *Coprococcus* amplify the same secretion axis, implying that microbial metabolites and bitter ligands can work in tandem to sustain incretin output late in life. The associations involving *Prevotella* were ambivalent: one edge connected the genus to higher *Tnf* expression, consistent with the pro-inflammatory potential of certain mucin-degrading strains;[52] however, other studies associate *P. copri* with succinate-driven GLP-1 stimulation and improved glycaemic control.[53]

Although *Sutterella* did not feature among the top network nodes, its abundance still fell as major *Tas2r* hubs rose, mirroring observations that this IgA-degrading genus is depleted in Chinese nonagenarians compared with younger elders.[54] Alongside the favourable Tas2R–*Bifidobacterium* and Tas2R–barrier associations, this inverse relationship suggests that bitter-receptor signalling may help steer the microbiota toward a longevity-aligned configuration.

Building on earlier work in diet-induced obesity, where the same 10-day, high-dose GSPE pulse given before the obesogenic challenge prevented weight gain, insulin resistance, low-grade inflammation and barrier leakiness for at least two months,[15] our current data show that an identical regimen delivered during late life delays or blunts several hallmarks of physiological ageing for more than eleven weeks after the last dose. Importantly, the one-off course (500 mg per kg per day) corresponds to a single-serving nutraceutical dose that is feasible in humans and has already been tested for safety and palatability.[23] Because efficacy is maintained without chronic re-dosing, strategically timed "polyphenol pulses" could represent a practical, compliance-friendly strategy to reinforce intestinal resilience; prospective human studies are now needed to determine how long such benefits persist and how frequently the pulses should be repeated. Furthermore, this translation to humans should also embrace a personalised framework. The sizeable allelic diversity in human TAS2Rs, together with wide interpersonal differences in gut–microbial

polyphenol metabolism, implies that pulse frequency, dose and even receptor-targeted polyphenol blends may need to be stratified by genotype and microbiome profile.[36,37] Such precision tailoring could optimise the sentinel-node function we describe here while avoiding over-supplementation in low responders.

Several caveats merit consideration. First, we quantified *Tas2r* transcripts rather than receptor protein or acute second-messenger flux. Because our goal was to determine whether a 10-day polyphenol intervention leaves a molecular footprint that is still detectable 11 weeks later, steady-state mRNA levels provide the most relevant read-out: durable shifts in gene expression are more likely to arise from chromatin remodelling, altered transcription-factor binding or non-coding-RNA regulation than from transient Ca^{2+} signalling. Future work should therefore pair transcriptomics with histone-mark and DNA-methylation profiling at the *Tas2r* loci to test for an epigenetic "memory" of the initial GSPE encounter. Second, the study used female rats only; sex-dependent differences in bitter sensitivity and in GSPE efficacy have been reported,[4,22] so replication in males is needed.

Finally, the partial-correlation network remains correlative in nature. While associative analyses can reveal meaningful relationships between variables, they are inherently limited in their ability to establish causality. Observed associations may be influenced by confounding factors, reverse causation, or coincidental correlations. To move beyond correlation, complementary mechanistic or interventional approaches are needed. These may include targeted receptor knock-out models or the use of antagonists to block receptor signalling, combined with gnotobiotic transfers or depletion of key genera such as *Bifidobacterium*, *Prevotella* and *Sutterella*. Such strategies will be essential to determine causality and to assess whether defined proanthocyanidin fractions can replicate the effects of the full GSPE mixture.

The present study was conducted in aged female subjects. However, sex is known to modulate bitter taste biology and polyphenol responses. Human mapping of gastrointestinal TAS2Rs has revealed sex-dependent differences in the ascending colon and age-related effects in the descending colon, suggesting region-specific regulation by sex hormones or sex-linked factors.[8] Population studies also report sex differences in bitter intensity phenotypes and responsiveness to PROP/thiourea, indicating upstream sensory variation.[4] In rodent models, GSPE pharmacokinetics—including absorption, tissue distribution, metabolism, and excretion—exhibit sex-dependent patterns.[55] Moreover, sex-specific microbiota–polyphenol interactions have been described, which may influence ligand exposure and receptor tone,[8] key components of our imprinting model. Future studies will replicate the pulse regimen in aged males, incorporating assessments of TAS2R expression, intestinal barrier integrity, and endocrine responses. Analyses will be stratified by microbiota composition and, where available, genotype.

Taken together, our data support an imprinting model of gut bitter sensing in aged female rats. Region-specific attenuation of intestinal *Tas2r* transcription in aged rats was accompanied by weaker epithelial barriers, dampened enteroendocrine signals, and microbiota shifts toward pro-inflammatory taxa. A brief, GSPE intervention, assessed 11 weeks after dosing, well beyond the expected clearance of parent flavanols, reinstated *Tas2r* expression in proximal segments, reshaped microbial associations, improved barrier read-outs and normalised hormone markers, even as several distal-colonic receptors remained down-modulated. These durable adaptations argue that early activation of mucosal bitter-taste pathways can reprogram host–microbiota interactions rather than requiring persistent ligand exposure. We propose that gut-expressed TAS2Rs function as sentinel nodes linking episodic dietary polyphenol intake to long-term metabolic and immune outcomes, and that strategically timed polyphenol "pulses" may offer a practical route to reinforce intestinal resilience and extend health span in ageing populations.

Author contributions

A. V.: writing – original draft, data curation, animal studies, sample processing, and sample analysis. M. D. S.: writing – review and editing. M. S. C.: animal studies, sample processing, and sample analysis. A. M. G.: animal studies, sample processing, and sample analysis. R. B. D.: conceptualization, formal analysis, and supervision. E. R. G.: research and conceptualization. M. P.: conceptualization, funding acquisition, and project administration. M. T. B.: research, conceptualization, and resources. A. A.: conceptualization, funding acquisition, project administration, and supervision. X. T.: conceptualization, writing – review & editing, formal analysis, and supervision.

Conflicts of interest

The authors declare that the research was conducted in the absence of any commercial or financial relationships that could be construed as a potential conflict of interest.

Data availability

Data for this article, including bitter taste receptor expression and metabolomics data, are available at the Repositori Institucional of Universitat Rovira i Virgili and can be accessed through https://repositori.urv.cat/estatic/PC0041/ca_DeptDSPC_Bioquimica_i_Biotecnologia.html.

Supplementary information (SI) is available and includes a list of all variables used in the study, categorized by topic, and Spearman correlation analyses between Tas2r gene expression across gastrointestinal segments. See DOI: https://doi.org/10.1039/d5fo03241e.

Acknowledgements

This study was funded by a grant PID2021-122636OB-I00 funded by MCIN/AEI/10.13039/501100011033/ and "ERDF A way of making Europe". This project has received funding from the Universitat Rovira i Virgili (URV). This work was supported by the Agència de Gestió d'Ajuts Universitaris i de Recerca (AGAUR), Departament de Recerca i Universitats de la Generalitat de Catalunya, under grant number 2021 SGR 00201. M. Sierra-Cruz and A. Miguéns-Gómez received a doctoral research grant from the Martí i Franquès programme of the Universitat Rovira i Virgili. M. Descamps-Solà and A. Vilalta received a doctoral research grant from the FI Joan Oró and FI-SDUR programmes, respectively, of the Generalitat de Catalunya. M. Pinent and X. Terra are Serra Húnter fellows. The authors would like to thank Niurka Llopiz for technical support.

References

1 M. Descamps-Solà, A. Vilalta, F. Jalsevac, M. T. Blay, E. Rodríguez-Gallego, M. Pinent, R. Beltrán-Debón, X. Terra and A. Ardévol, Bitter taste receptors along the gastrointestinal tract: comparison between humans and rodents, *Front. Nutr.*, 2023, **10**, 1215889.

2 M. O. Welcome, D. Dogo and N. E. Mastorakis, Cellular mechanisms and molecular pathways linking bitter taste receptor signalling to cardiac inflammation, oxidative stress, arrhythmia and contractile dysfunction in heart diseases, *Inflammopharmacology*, 2022, **31**, 89–117.

3 M. Behrens and T. Lang, Extra-Oral Taste Receptors-Function, Disease, and Perspectives, *Front. Nutr.*, 2022, **9**, 881177.

4 R. Barragán, O. Coltell, O. Portolés, E. M. Asensio, J. V. Sorlí, C. Ortega-Azorín, J. I. González, C. Sáiz, R. Fernández-Carrión, J. M. Ordovas and D. Corella, Bitter, Sweet, Salty, Sour and Umami Taste Perception Decreases with Age: Sex-Specific Analysis, Modulation by Genetic Variants and Taste-Preference Associations in 18 to 80 Year-Old Subjects, *Nutrients*, 2018, **10**, 1539.

5 M. Narukawa, A. Kamiyoshihara, M. Kawae, R. Kohta and T. Misaka, Analysis of aging-dependent changes in taste sensitivities of the senescence-accelerated mouse SAMP1, *Exp. Gerontol.*, 2018, **113**, 64–73.

6 H. T. T. Tran, C. Herz, P. Ruf, R. Stetter and E. Lamy, Human T2R38 bitter taste receptor expression in resting and activated lymphocytes, *Front. Immunol.*, 2018, **9**, 418485.

7 D. Whissell-Buechy, Effects of age and sex on taste sensitivity to phenylthiocarbamide (PTC) in the Berkeley Guidance sample, *Chem. Senses*, 1990, **15**, 39–57.

8 F. Jalševac, M. Descamps-Solà, C. Grau-Bové, H. Segú, T. Auguet, F. X. Avilés-Jurado, F. Balaguer, R. Jorba, R. Beltrán-Debón, M. T. Blay, X. Terra Barbadora, M. Pinent and A. Ardévol, Profiling bitter taste receptors (TAS2R) along the gastrointestinal tract and their influence on enterohormone secretion. Gender- and age-related effects in the colon, *Front. Endocrinol.*, 2024, **15**, DOI: 10.3389/FENDO.2024.1436580.

9 F. Jalševac, H. Segú, F. Balaguer, T. Ocaña, R. Moreira, L. Abad-Jordà, J. Gràcia-Sancho, A. Fernández-Iglesias, C. Andres-Lacueva, M. Martínez-Huélamo, R. Beltran-Debon, E. Rodríguez-Gallego, X. Terra, A. Ardévol and M. Pinent, TAS2R5 and TAS2R38 are bitter taste receptors whose colonic expressions could play important roles in age-associated processes, *J. Nutr. Biochem.*, 2025, **140**, DOI: 10.1016/j.jnutbio.2025.109872.

10 M. Trius-Soler and J. J. Moreno, Bitter taste receptors: Key target to understand the effects of polyphenols on glucose and body weight homeostasis. Pathophysiological and pharmacological implications, *Biochem. Pharmacol.*, 2024, **228**, DOI: 10.1016/j.bcp.2024.116192.

11 N. Gonzalez-Abuin, M. Pinent, A. Casanova-Marti, L. Arola, M. Blay and A. Ardevol, Procyanidins and their healthy protective effects against type 2 diabetes, *Curr. Med. Chem.*, 2015, **22**, 39–50.

12 C. González-Quilen, K. Gil-Cardoso, I. Ginés, R. Beltrán-Debón, M. Pinent, A. Ardévol, X. Terra and M. T. Blay, Grape-Seed Proanthocyanidins are Able to Reverse Intestinal Dysfunction and Metabolic Endotoxemia Induced by a Cafeteria Diet in Wistar Rats, *Nutrients*, 2019, **11**(5), DOI: 10.3390/NU11050979.

13 K. Gil-Cardoso, I. Ginés, M. Pinent, A. Ardévol, M. Blay and X. Terra, The co-administration of proanthocyanidins and an obesogenic diet prevents the increase in intestinal permeability and metabolic endotoxemia derived to the diet, *J. Nutr. Biochem.*, 2018, **62**, 35–42.

14 K. Gil-Cardoso, I. Ginés, M. Pinent, A. Ardévol, M. Blay and X. Terra, Effects of flavonoids on intestinal inflammation, barrier integrity and changes in gut microbiota during diet-induced obesity, *Nutr. Res. Rev.*, 2016, **29**, 234–248.

15 I. Ginés, K. Gil-Cardoso, J. Serrano, À. Casanova-Martí, M. T. Blay, M. Pinent, A. Ardévol and X. Terra, Effects of an Intermittent Grape-Seed Proanthocyanidin (GSPE) Treatment on a Cafeteria Diet Obesogenic Challenge in Rats, *Nutrients*, 2018, **10**, 315.

16 K. Gil-Cardoso, R. Comitato, I. Ginés, A. Ardévol, M. Pinent, F. Virgili, X. Terra and M. Blay, Protective Effect of Proanthocyanidins in a Rat Model of Mild Intestinal Inflammation and Impaired Intestinal Permeability Induced by LPS, *Mol. Nutr. Food Res.*, 2019, **63**(8), DOI: 10.1002/mnfr.201800720.

17 À. Casanova-Martí, J. Serrano, M. T. Blay, X. Terra, A. Ardévol and M. Pinent, Acute selective bioactivity of grape seed proanthocyanidins on enteroendocrine secretions in the gastrointestinal tract, *Food Nutr. Res.*, 2017, **61**(1), DOI: 10.1080/16546628.2017.1321347.

18 D. Pajuelo, H. Quesada, S. Díaz, A. Fernández-Iglesias, A. Arola-Arnal, C. Bladé, J. Salvadó and L. Arola, Chronic

dietary supplementation of proanthocyanidins corrects the mitochondrial dysfunction of brown adipose tissue caused by diet-induced obesity in Wistar rats, *Br. J. Nutr.*, 2012, **107**, 170–178.

19 I. Baiges, J. Palmfeldt, C. Bladé, N. Gregersen and L. Arola, Lipogenesis is decreased by grape seed proanthocyanidins according to liver proteomics of rats fed a high fat diet, *Mol. Cell. Proteomics*, 2010, **9**, 1499–1513.

20 M. Sierra-Cruz, A. Miguéns-Gómez, C. Grau-Bové, E. Rodríguez-Gallego, M. Blay, M. Pinent, A. Ardévol, X. Terra and R. Beltrán-Debón, Grape-Seed Proanthocyanidin Extract Reverts Obesity-Related Metabolic Derangements in Aged Female Rats, *Nutrients*, 2021, **13**(6), DOI: 10.3390/NU13062059.

21 A. Miguéns-Gómez, M. Sierra-Cruz, A. M. Pérez-Vendrell, E. Rodríguez-Gallego, R. Beltrán-Debón, X. Terra, A. Ardévol and M. Pinent, Differential effects of a cafeteria diet and GSPE preventive treatments on the enterohormone secretions of aged vs. young female rats, *Food Funct.*, 2022, **13**(20), DOI: 10.1039/D2FO02111K.

22 C. Grau-Bové, M. Sierra-Cruz, A. Miguéns-Gómez, E. Rodríguez-Gallego, R. Beltrán-Debón, M. Blay, X. Terra, M. Pinent and A. Ardévol, A ten-day grape seed procyanidin treatment prevents certain ageing processes in female rats over the long term, *Nutrients*, 2020, **12**, 1–12.

23 M. Sierra-Cruz, A. Vilalta, A. Miguéns-Gómez, H. Park, E. Rodríguez-Gallego, M. T. Blay, A. Ardévol, M. Pinent, J. Behmoaras, R. Beltrán-Debón and X. Terra, Grape Seed Proanthocyanidins: A Potential Microbiome-Targeted Intervention for Healthy Aging in Rats, *Mol. Nutr. Food Res.*, 2025, **69**(18), DOI: 10.1002/MNFR.70150.

24 M. Margalef, Z. Pons, F. I. Bravo, B. Muguerza and A. Arola-Arnal, Tissue distribution of rat flavanol metabolites at different doses, *J. Nutr. Biochem.*, 2015, **26**(10), 987–995, DOI: 10.1016/j.jnutbio.2015.04.006.

25 M. Margalef, Z. Pons, L. Iglesias-Carres, F. I. Bravo, B. Muguerza and A. Arola-Arnal, Lack of Tissue Accumulation of Grape Seed Flavanols after Daily Long-Term Administration in Healthy and Cafeteria-Diet Obese Rats, *J. Agric. Food Chem.*, 2015, **63**, 9996–10003.

26 S. V. Wu, N. Rozengurt, M. Yang, S. H. Young, J. Sinnett-Smith and E. Rozengurt, Expression of bitter taste receptors of the T2R family in the gastrointestinal tract and enteroendocrine STC-1 cells, *Proc. Natl. Acad. Sci. U. S. A.*, 2002, **99**, 2392–2397.

27 T. Kamila and K. Agnieszka, An update on extra-oral bitter taste receptors, *J. Transl. Med.*, 2021, **19**, 1–33.

28 Q. Wang, K. I. Liszt and I. Depoortere, Extra-oral bitter taste receptors: New targets against obesity?, *Peptides*, 2020, **127**, DOI: 10.1016/J.PEPTIDES.2020.170284.

29 M. Behrens, S. Prandi and W. Meyerhof, Taste Receptor Gene Expression Outside the Gustatory System, *Top. Med. Chem.*, 2014, **23**, 1–34.

30 W. Meyerhof, C. Batram, C. Kuhn, A. Brockhoff, E. Chudoba, B. Bufe, G. Appendino and M. Behrens, The molecular receptive ranges of human TAS2R bitter taste receptors, *Chem. Senses*, 2010, **35**, 157–170.

31 K. Lossow, S. Hübner, N. Roudnitzky, J. P. Slack, F. Pollastro, M. Behrens and W. Meyerhof, Comprehensive Analysis of Mouse Bitter Taste Receptors Reveals Different Molecular Receptive Ranges for Orthologous Receptors in Mice and Humans, *J. Biol. Chem.*, 2016, **291**, 15358–15377.

32 K. S. Kim, J. M. Egan and H. J. Jang, Denatonium induces secretion of glucagon-like peptide-1 through activation of bitter taste receptor pathways, *Diabetologia*, 2014, **57**, 2117–2125.

33 C. Grau-Bové, A. Miguéns-Gómez, C. González-Quilen, J. A. Fernández-López, X. Remesar, C. Torres-Fuentes, J. Ávila-Román, E. Rodríguez-Gallego, R. Beltrán-Debón, M. T. Blay, X. Terra, A. Ardévol and M. Pinent, Modulation of Food Intake by Differential TAS2R Stimulation in Rat, *Nutrients*, 2020, **12**, 3784.

34 S. Janssen, J. Laermans, P.-J. Verhulst, T. Thijs, J. Tack and I. Depoortere, Bitter taste receptors and α-gustducin regulate the secretion of ghrelin with functional effects on food intake and gastric emptying., *Proc. Natl. Acad. Sci. U. S. A.*, 2011, **108**, 2094–2099.

35 K. I. Liszt, Q. Wang, M. Farhadipour, A. Segers, T. Thijs, L. Nys, E. Deleus, B. van der Schueren, C. Gerner, B. Neuditschko, L. J. Ceulemans, M. Lannoo, J. Tack and I. Depoortere, Human intestinal bitter taste receptors regulate innate immune responses and metabolic regulators in obesity, *J. Clin. Invest.*, 2022, **132**(3), DOI: 10.1172/JCI144828.

36 D. R. Reed and A. Knaapila, Genetics of Taste and Smell: Poisons and Pleasures, *Prog. Mol. Biol. Transl. Sci.*, 2010, **94**, 213–240.

37 M. V. Selma, J. C. Espín and F. A. Tomás-Barberán, Interaction between phenolics and gut microbiota: Role in human health, *J. Agric. Food Chem.*, 2009, **57**, 6485–6501.

38 J. I. Ottaviani, C. Kwik-Uribe, C. L. Keen and H. Schroeter, Intake of dietary procyanidins does not contribute to the pool of circulating flavanols in humans, *Am. J. Clin. Nutr.*, 2012, **95**, 851–858.

39 A. Miguéns-Gómez, M. Sierra-Cruz, M. T. Blay, E. Rodríguez-Gallego, R. Beltrán-Debón, X. Terra, M. Pinent and A. Ardévol, GSPE Pre-Treatment Exerts Long-Lasting Preventive Effects against Aging-Induced Changes in the Colonic Enterohormone Profile of Female Rats, *Int. J. Mol. Sci.*, 2023, **24**(9), DOI: 10.3390/IJMS24097807.

40 M. Sierra-Cruz, A. Miguéns-Gómez, C. Grau-Bové, E. Rodríguez-Gallego, M. Blay, M. Pinent, A. Ardévol, X. Terra and R. Beltrán-Debón, Grape-seed proanthocyanidin extract reverts obesity-related metabolic derangements in aged female rats, *Nutrients*, 2021, **13**(6), DOI: 10.3390/nu13062059.

41 A. Miguéns-Gómez, M. Sierra-Cruz, A. M. Pérez-Vendrell, E. Rodríguez-Gallego, R. Beltrán-Debón, X. Terra, A. Ardévol and M. Pinent, Differential effects of a cafeteria diet and GSPE preventive treatments on the enterohor-

mone secretions of aged vs. young female rats, *Food Funct.*, 2022, **13**, 10491–10500.

42 K. Takeuchi, K. Yoshii and Y. Ohtubo, Age-related electrophysiological changes in mouse taste receptor cells, *Exp. Physiol.*, 2021, **106**, 519–531.

43 O. Coltell, J. V. Sorlí, E. M. Asensio, R. Fernández-Carrión, R. Barragán, C. Ortega-Azorín, R. Estruch, J. I. González, J. Salas-Salvadó, S. Lamon-Fava, A. H. Lichtenstein and D. Corella, Association between taste perception and adiposity in overweight or obese older subjects with metabolic syndrome and identification of novel taste-related genes, *Am. J. Clin. Nutr.*, 2019, **109**, 1709–1723.

44 S. Bayer, A. I. Mayer, G. Borgonovo, G. Morini, A. Di Pizio and A. Bassoli, Chemoinformatics View on Bitter Taste Receptor Agonists in Food, *J. Agric. Food Chem.*, 2021, **69**, 13916–13924.

45 Y. Su, H. Jie, Q. Zhu, X. Zhao, Y. Wang, H. Yin, S. Kumar Mishra and D. Li, Effect of Bitter Compounds on the Expression of Bitter Taste Receptor T2R7 Downstream Signaling Effectors in cT2R7 /pDisplay-G α 16/gust44/pcDNA3.1 (+) Cells, *BioMed Res. Int.*, 2019, DOI: 10.1155/2019/6301915.

46 I. Ginés, K. Gil-Cardoso, J. Serrano, À. Casanova-Marti, M. Lobato, X. Terra, M. T. Blay, A. Ardévol and M. Pinent, Proanthocyanidins limit adipose accrual induced by a cafeteria diet, several weeks after the end of the treatment, *Genes*, 2019, **10**(8), DOI: 10.3390/genes10080598.

47 D. Campa, F. de Rango, M. Carrai, P. Crocco, A. Montesanto, F. Canzian, G. Rose, C. Rizzato, G. Passarino and R. Barale, Bitter taste receptor polymorphisms and human aging, *PLoS One*, 2012, **7**(11), DOI: 10.1371/JOURNAL.PONE.0045232.

48 M. Melis, A. Errigo, R. Crnjar, G. M. Pes and I. Tomassini Barbarossa, TAS2R38 bitter taste receptor and attainment of exceptional longevity, *Sci. Rep.*, 2019, **9**(1), DOI: 10.1038/S41598-019-54604-1.

49 R. Toumi, I. Soufli, H. Rafa, M. Belkhelfa, A. Biad and C. Touil-Boukoffa, Probiotic bacteria lactobacillus and bifidobacterium attenuate inflammation in dextran sulfate sodium-induced experimental colitis in mice, *Int. J. Immunopathol. Pharmacol.*, 2014, **27**, 615–627.

50 T. Sumitomo, M. Nakata, M. Higashino, Y. Jin, Y. Terao, Y. Fujinaga and S. Kawabata, Streptolysin S Contributes to Group A Streptococcal Translocation across an Epithelial Barrier, *J. Biol. Chem.*, 2010, **286**, 2750.

51 Y. Chen, M. Zhang and F. Ren, A Role of Exopolysaccharide Produced by Streptococcus thermophilus in the Intestinal Inflammation and Mucosal Barrier in Caco-2 Monolayer and Dextran Sulphate Sodium-Induced Experimental Murine Colitis, *Molecules*, 2019, **24**, 513.

52 N. A. Abdelsalam, S. M. Hegazy and R. K. Aziz, The curious case of Prevotella copri, *Gut Microbes*, 2023, **15**(2), DOI: 10.1080/19490976.2023.2249152.

53 C. Yang, R. Lan, L. Zhao, J. Pu, D. Hu, J. Yang, H. Zhou, L. Han, L. Ye, D. Jin, J. Xu and L. Liu, Prevotella copri alleviates hyperglycemia and regulates gut microbiota and metabolic profiles in mice, *mSystems*, 2024, **9**, e00532–e00524.

54 J. Liu, W. J. Wang, G. F. Xu, Y. X. Wang, Y. Lin, X. Zheng, S. H. Yao and K. H. Zheng, Does Microbiome Contribute to Longevity? Compositional and Functional Differences in Gut Microbiota in Chinese Long-Living (>90 Years) and Elderly (65–74 Years) Adults, *OMICS*, 2024, **28**, 461–469.

55 M. Margalef, Z. Pons, L. Iglesias-Carres, L. Arola, B. Muguerza and A. Arola-Arnal, Gender-related similarities and differences in the body distribution of grape seed flavanols in rats, *Mol. Nutr. Food Res.*, 2016, **60**, 760–772.